

# Achieving Downstream Fairness with Geometric Repair

Kweku Kwegyir-Aggrey<sup>1,2</sup>, Jessica Dai<sup>1</sup>, John P. Dickerson<sup>1,3</sup>, and Keegan Hines<sup>1</sup>

<sup>1</sup>Arthur AI

<sup>2</sup>Department of Computer Science, Brown University

<sup>3</sup>Department of Computer Science, University of Maryland - College Park

June 16, 2022

## Abstract

We study a fair machine learning (ML) setting where an ‘upstream’ model developer is tasked with producing a fair ML model that will be used by several similar but distinct ‘downstream’ users. This setting introduces new challenges that are unaddressed by many existing fairness interventions, echoing existing critiques that current methods are not broadly applicable across the diversifying needs of real-world fair ML use cases. To this end, we address the up/down stream setting by adopting a distributional-based view of fair classification. Specifically, we introduce a new fairness definition, distributional parity, that measures disparities in the distribution of outcomes across protected groups, and present a post-processing method to minimize this measure using techniques from optimal transport. We show that our method is able that creates fairer outcomes for all downstream users, across a variety of fairness definitions, and works at inference time on unlabeled data. We verify this claim experimentally, through comparison to several similar methods and across four benchmark tasks. Ultimately we argue that fairer classification outcomes can be produced through the development of setting-specific interventions.

# Contents

<b>1</b>	<b>Introduction</b>	<b>2</b>
1.1	Contributions . . . . .	2
<b>2</b>	<b>Preliminaries</b>	<b>3</b>
2.1	Fairness Preliminaries . . . . .	3
2.2	Wasserstein Preliminaries . . . . .	4
<b>3</b>	<b>Distributional Parity</b>	<b>5</b>
3.1	Distributional Parity and Label-Dependent Metrics . . . . .	6
3.2	Additional Related Work . . . . .	7
<b>4</b>	<b>Geometric Repair</b>	<b>7</b>
4.1	Properties of Geometric Repair . . . . .	8
4.2	Minimizing Distributional Disparity . . . . .	9
4.2.1	Wasserstein Geodesics . . . . .	9
4.2.2	Fairness Metrics as Functionals . . . . .	10
4.2.3	Displacement Convexity . . . . .	11
4.2.4	Post-Processing for Distributional Parity . . . . .	11
<b>5</b>	<b>Experiments</b>	<b>12</b>
5.1	Results . . . . .	13
<b>6</b>	<b>Discussion</b>	<b>13</b>
<b>A</b>	<b>Helping Results</b>	<b>17</b>
<b>B</b>	<b>Proofs</b>	<b>17</b>
B.1	Proof of Proposition 1 . . . . .	17
B.2	Proof of Proposition 2 . . . . .	18
B.3	Proof of Proposition 3 . . . . .	18
B.4	Proof of Remark 4.1 . . . . .	18
B.5	Proof of Lemma 4.1 . . . . .	18
B.6	Proof of Proposition 4 . . . . .	19
B.7	Proof of Lemma 4.2 . . . . .	19
B.8	Proof of Lemma A.1 . . . . .	19
B.9	Proof of Theorem 3 . . . . .	20
<b>C</b>	<b>Experimental details</b>	<b>20</b>
C.1	Experimental setup . . . . .	20
C.2	Datasets . . . . .	21
<b>D</b>	<b>Usability</b>	<b>22</b>
D.1	Suitability . . . . .	22

# 1 Introduction

A common critique of fair machine learning algorithms is that they do not center real-world usage [Hof19, SBF<sup>+</sup>19]. In this work, we study a problem that arises from the gap between the design of “fair” machine learning interventions in the lab, and their deployment in the real world. Specifically, we consider a commercial context, where there are many “downstream” clients who are interested in using a fair supervised machine-learning model for related/similar prediction tasks, but do not have the expertise, data, or resources to train the model themselves. As a result, they delegate the computation to some “upstream” ML model developer [BKN<sup>+</sup>17, DIJ20].

**Example 1.1.** A large company has created a model to predict the likelihood of having a severe illness (e.g. one of the systems in [PSRA<sup>+</sup>20]). It is being used in several hospitals in areas that serve similar populations. They wish to ensure that their model is not discriminating across some minority group in the following use cases. At these hospitals, outreach teams wish to notify all the patients that are more likely than not to have the illness, and therefore use a “low” decision threshold between 0.3 and 0.5 to determine which patients to contact. The clinical teams, on the other hand, depending on the hospital’s resources, have varying resources to treat patients, and therefore use a much wider set of thresholds, falling anywhere between 0.55 and 0.9, to determine which patients to treat.

In this example, we see that variety in downstream usage forms a key bottleneck in the production of a fair model for the upstream developer: each downstream user will need to use the same model, but with different thresholds due to minor differences in individual use cases. For example, different costs associated with for example, true and false positives [ZVR<sup>+</sup>17, ABD<sup>+</sup>18, HC20] can lead to several downstream users employing different thresholds for the same classification task. Furthermore, there are an infinite number of thresholds between e.g. 0.3 and 0.5, with each resulting in different (potentially) unfair consequences for the downstream user to have to choose between. This prevents the upstream developer from optimizing for fairness at a specific threshold, or even a small number of thresholds, since the “right” threshold is not known a-priori.

One solution that has been proposed to address this problem is to mitigate bias for all possible thresholds at once. The idea behind the all-threshold solution is the following: if a model is fair at all thresholds at once, then it will remain fair for any downstream, threshold-dependent, use case. Some existing works have attempted to meet this all-threshold goal, however many suffer from strict modeling assumptions [CW20] or are limited to only attaining demographic parity [CDH<sup>+</sup>20a, CDH<sup>+</sup>20b, FFM<sup>+</sup>15, JPS<sup>+</sup>20, GDBFL19, GLR20], a naive definition of fairness, at every threshold. Notably, this limitation excludes some popular choices of fairness definitions, such as Equalized Odds or Equal Opportunity [HPS16], that are *label dependent* in the sense that they require knowledge of a ground truth label  $Y$ , which may not be available in downstream settings where data is often unlabeled [CKM<sup>+</sup>19].

In this work, we address these limitations by proposing a flexible post-processing method which can attain all-threshold fairness for a wide class of label dependent and independent fairness metrics including, but not limited to demographic parity, equalized odds, and equal opportunity. The key idea underlying our approach, is that all-threshold fairness is easy to achieve when the distributions of model outputs *prior* to thresholding are identically distributed, across protected groups. To service this intuition, we present a new measure of fairness called distributional (dis)parity which measures differences between these pre-thresholding output distributions and then leverage our new fairness measure to propose a method for attaining fairness across all thresholds, or in other words, for removing distributional disparity. Our method centers around techniques from Optimal Transport, which is a statistical method for transforming probability distributions and measuring the differences between them. We formally state our contributions as follows.

## 1.1 Contributions

We introduce a post-processing algorithm that addresses this upstream/downstream setting by minimizing rate disparities in a fairness metric across **all-thresholds**. Explicitly: **(i.)** We formalize distributional parity, illustrate its connection to group score distributions, and show that attaining distributional parity minimizes rate disparities across all thresholds in our up/downstream setting. **(ii.)** We present our post-processing (Algorithm 1) which is rooted in the geometric repair technique as introduced in [FFM<sup>+</sup>15, CS20]. We

demonstrate that geometric repair meets several key desiderata in the upstream/downstream setting, and show theoretically that it can be used to maximize distributional parity. Furthermore, our algorithm can post process any real valued regressor, and can be applied in practice on unlabeled data (Algorithm 1). (iii.) We make a theoretical contribution at the intersection of optimal transport and fairness by proposing a new framework for computing fair distributions through a novel convexity result on fairness metrics over probability distributions (Lemma 4.2). We conclude by showing that our approach outperforms related approaches across four benchmark fair prediction tasks.

## 2 Preliminaries

Allow  $X \subseteq \mathbb{R}^d$  to be the feature space,  $Y = \{0, 1\}$  a set of labels, and  $\mathcal{G}$  be the set of binary protected attributes where  $g$  is the majority group and  $g'$  the minority group. Similarly, let  $D = \{(x_i, g_i, y_i)\}_{i=1}^N$  be a dataset consisting of features  $x_i \in \mathcal{X}$ , a protected attribute  $g_i \in \mathcal{G}$ , and a classification label  $y_i \in Y$ , with each drawn from some unknown, underlying distribution. We'll use boldfaced  $\mathbf{X}, \mathbf{G}, \mathbf{Y}$  to denote the associated random variables. Let  $\Omega \subseteq [0, 1]$  be a closed subset and  $f : X \times \mathcal{G} \rightarrow \Omega$  a regressor that estimates the likelihood some  $(x, g)$  attains the outcome denoted by the positive classification label i.e.

$$f(x, g) = \Pr(\mathbf{Y} = 1 | \mathbf{X} = x, \mathbf{G} = g)$$

We often refer to the probabilities output by  $f(x, g)$  as *scores* given that they “rank” the  $(x, g)$  based on their predicted likelihood of attaining the  $Y = 1$  outcome. When the regressor is clear from context, we denote these scores  $s_i = f(x_i, g_i)$  with random variable  $\mathbf{S}$ . Discrete decisions/classifications (which are instantiated from these scores) are denoted  $\hat{Y}$ . We are primarily concerned with a binary classification setting, so we let  $\hat{Y} = 1$  denote the allocation of some intervention, and  $\hat{Y} = 0$  will denote the opposite. The allocation of the intervention is determined by applying a threshold  $\tau \in [0, 1]$  to regressor scores i.e.  $\hat{y}_i = \mathbf{1}_{s_i \geq \tau}$ .

One type of distribution that we will frequently refer to is the distribution of scores produced by the regressor, but for a specific group – we call these the *groupwise* score distributions or *group-conditional* score distributions. Let  $\mathcal{P}_1(\Omega)$  denote the set of probability measures with finite first order moments on  $\Omega$ . The distribution of scores for a group  $g$  is nothing more than  $\Pr(\mathbf{S} = s | \mathbf{G} = g)$  and has random variable  $\mathbf{S}_g$ . These probabilities are associated with some measure  $\mu \in \mathcal{P}_1(\Omega)$  where e.g.  $\mu_{\mathbf{S}}$  is the measure associated with  $\mathbf{S}$ . The cumulative distribution function of  $\mu_{\mathbf{S}_g}$  is denoted  $F_g(\tau) = \mu_{\mathbf{S}_g}([\infty, \tau))$  and because of the following assumption, has a well defined inverse  $F_g^{-1}$ .

**Assumption 2.1.** Any measure  $\mu \in \mathcal{P}_1(\Omega)$  is non-atomic with finite first moments, and absolutely continuous with respect to the Lebesgue measure.

Non-atomicity and finite-moment assumptions are standard in papers which study optimal transport of univariate distributions such as [AC11, CS20] (this can also be seen throughout [San15]). The key reason for the non-atomicity assumption is the following: if a distribution's measure is non-atomic then its CDF strictly non-decreasing, which means the inverse CDF of that same distribution is well defined and also non-decreasing. As we will see in Section 2.2 this is crucial for establishing well-defined optimal transport maps in the one-dimensional setting. We will also see that the finite-moment assumption is necessary to define the Wasserstein Distance, which is an optimal-transport based notion of statistical distance over these measures. Assuming absolute continuity with respect to the Lebesgue measure is also required in this setup, as absolute continuity implies the existence of probability density functions which are required to prove our main result.

### 2.1 Fairness Preliminaries

In this work, we measure fairness using familiar measures of group fairness namely, True Positive Rate (TPR), False Positive Rate (FPR), and Positive Rate (PR). These rates correspond to popular fairness definitions such as Equal Opportunity (TPR Parity), Equalized Odds (TPR and FPR Parity) [HPS16], and Demographic Parity (PR Parity) [CKP09]. A classifier is said to be fair if these measures perform equally well across the identified protected groups, i.e. if the true positive rates for two groups are similar or equal, then the classifier

is fair (under TPR parity). We'll denote the PR of  $f$  at a threshold  $\tau$  as

$$PR_g^f(\tau) = \Pr[\mathbf{S} \geq \tau | \mathbf{G} = g]$$

and the TPR, and FPR as

$$TPR_g^f(\tau) = \Pr[\mathbf{S} \geq \tau | Y = 1, \mathbf{G} = g]; \quad FPR_g^f = \Pr[\mathbf{S} \geq \tau | Y = 0, \mathbf{G} = g]$$

Let this set of rates<sup>1</sup> be denoted with  $\Gamma = \{PR, TPR, FPR\}$ , and when referencing an arbitrary rate in this set, we'll use  $\gamma \in \Gamma$ . We'll also call TPR and FPR *label dependent* metrics, because of their reliance on a label  $Y$ , and for the same reason we call PR *label-independent*. Although the difference is subtle, we make this label independent/dependent distinction for ease of exposition; in Section 3 this difference will be very useful for explaining the limitations of current approaches for all-threshold fairness.

## 2.2 Wasserstein Preliminaries

The Wasserstein distance is a metric which measures the differences between probability distributions by measuring the *cost* of transforming one distribution into another—i.e. if this transportation is costly, then the Wasserstein distance between the two distributions will be large. For measures  $\mu, \nu \in \mathcal{P}_p(\Omega)$  with finite  $p$ th moments, and where  $\Omega$  is endowed with a distance  $d(x, y) = |x - y|^p$  for all  $x, y \in \Omega$ , the Wasserstein distance is computed

$$\mathcal{W}_p(\mu, \nu) := \inf_{\pi \in \Pi(\mu, \nu)} \left( \int_{\Omega} d(x, y)^p \pi(x, y) \right)^{\frac{1}{p}}$$

where  $\Pi(\mu, \nu)$  is the set of all measures over  $\Omega \times \Omega$  with marginals  $\mu, \nu$ . In this work however, we only consider the Wasserstein-1 Distance, which admits a closed form computation

$$\mathcal{W}_1(\mu, \nu) = \int_{\Omega} |F_{\mu}^{-1}(\omega) - F_{\nu}^{-1}(\omega)| d\omega. \quad (1)$$

This straightforward solution comes from the fact that for univariate measures, the Wasserstein-1 distance computation can be simplified through the use of a **transport plan**, which is especially well defined in the univariate setting. A transport plan is a function  $T : \Omega \rightarrow \Omega$  subject to the following constraint: if the elements in the pre-image of  $T$  have measure  $\mu$ , then the output of  $T$  must have measure  $\nu$ , or said differently, if  $T$  is the transport plan from  $\mu \rightarrow \nu$  then  $\nu(A) = \mu(T^{-1}(A))$  for all measurable  $A \subseteq \Omega$ . The measure resulting from using  $T$  to transport mass from  $\mu \rightarrow \nu$  under this constraint is called the push forward of  $\mu$  and is denoted  $T_{\#}\mu = \nu$ . Should we let  $\mathcal{T}$  be the set of transportation plans, the Wasserstein-1 distance can be alternatively computed as

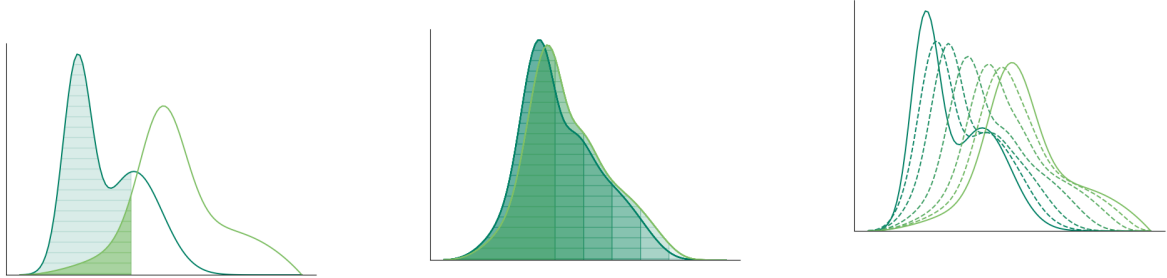
$$\mathcal{W}_1(\mu, \nu) := \inf_{T \in \mathcal{T}} \int_{\Omega} c(\omega, T(\omega)) d\mu(\omega) \quad \text{with} \quad T_{\#}\mu = \nu \quad (2)$$

where the cost minimizing plan that obeys push-forward constraints is called the optimal transport plan. For univariate non-atomic measures, we can compute this transport plan using only the cdf's and inverse cdf's of measures in question.

**Remark 2.1.** For non-atomic measures  $\mu, \nu \in \mathcal{P}_1(\Omega)$ , the optimal transport plan  $T$  from  $\mu \rightarrow \nu$  is a non-decreasing function and is computed  $T(\omega) = F_{\nu}^{-1}(F_{\mu}(\omega))$  where  $\omega \in \Omega$  ([San15] Theorem 2.5).

Using this distance, we can evoke familiar geometric concepts, but over probability distributions. Specifically, we can compose a “weighted average” of distributions, in a fashion very similar to a weighted average over real numbers. This weighted average over distributions is called the Wasserstein barycenter.

**Definition 2.1.** The Wasserstein-1 barycenter of two measures  $\mu_1, \mu_2 \in \mathcal{P}_1(\Omega)$  and  $\alpha \in [0, 1]$  is  $\nu^* := \arg \min_{\nu \in \mathcal{P}_1(\Omega)} \alpha \mathcal{W}_1(\mu_1, \nu) + (1 - \alpha) \mathcal{W}_1(\mu_2, \nu)$ .



(a) Difference in the shaded area between curves shows disparity in some  $\gamma$  at a single threshold.

(b) These curves nearly overlap, with both curves having similar area to the right of every threshold depicted, thereby having little  $\gamma$  disparities.

(c) To achieve distributional parity, we interpolate between groupwise score distributions along their barycenters. These are visualized via the dotted curves which are the various barycenters of the distributions.

Figure 1: An illustration of distributional parity and its relationship to the groupwise score distributions. Our method relies on interpolate between distributions to achieve distributional parity

### 3 Distributional Parity

In this section, we demonstrate how to analyze the fair performance of a regressor with respect to its groupwise score distributions, and also how this analysis can help us achieve "all-threshold" fairness guarantees as motivated in Section 1. To begin, consider a supervised fair classification model which consists of a regressor  $f$  thresholded with a  $\tau \in [0, 1]$ . Most classification based fairness notions are based on the joint distribution of binary decisions, labels, and attributes  $(\hat{\mathbf{Y}}, \mathbf{Y}, \mathbf{G})$  [BHN19]. However, by recalling that  $\hat{\mathbf{Y}}$  is produced by thresholding the output of a regressor, we can equivalently view this distribution as  $(\mathbb{1}_{S \geq \tau}, \mathbf{Y}, \mathbf{G})$  where  $S$  encodes distribution of scores before thresholding. An immediate consequence of this equivalence is that creating parity in decisions  $\hat{\mathbf{Y}}$  for all thresholds across groups, requires  $S_g, S_{g'}$  to be distributed similarly. The reason for this, is that if the two groupwise score distributions are identically distributed, then  $\Pr(S_g = s) = \Pr(S_{g'} = s)$  for all scores, meaning that groupwise rates will also be equal after a threshold is applied, that is  $\mathbb{1}_{S_g \geq \tau} = \mathbb{1}_{S_{g'} \geq \tau}$ . Alternatively, we can validate the conditions where all-threshold rate parity occurs through the language of statistical distances. That is, under a suitable statistical distance,  $S_g = S_{g'}$  is the same as vanishing said statistical distance between the corresponding measures  $\mu_{S_g}, \mu_{S_{g'}}$ . If there is no statistical distance between  $\mu_{S_g}, \mu_{S_{g'}}$ , then surely rate parity across all thresholds is achieved as we can show via the following proposition that this condition is equivalent to  $\Pr(S_g \geq \tau) = \Pr(S_{g'} \geq \tau)$  for all  $\tau \in [0, 1]$ . We illustrate this concept in Figure 1.

**Proposition 1.** The Wasserstein-1 distance (Eqn 1) between two measures is exactly equal to the average difference in positive rates between those distributions, where this average is taken uniformly across all thresholds,

$$\mathcal{W}_1(\mu_{S_g}, \mu_{S_{g'}}) = \mathbb{E}_{\tau \sim U(\Omega)} |PR_g^f(\tau) - PR_{g'}^f(\tau)| \quad (3)$$

where  $U(\Omega)$  denotes the uniform distribution over  $\Omega$ .

This equality demonstrates that measuring the average difference in a fairness metric across all thresholds exactly recovers the Wasserstein distance between the groupwise score distributions. Additionally, this relationship also hints that using techniques which reduce the Wasserstein-1 distance between distributions, will be helpful in achieving our all-threshold goal. That is, if the Wasserstein distance between two groupwise score distributions is zero, then there will be no classification disparity between these distributions at any threshold, as the difference in some metric will also be zero at all thresholds, according to the above proposition.

<sup>1</sup>Our results also extend to the "negative" versions of these rates, which can be easily recovered by considering  $\Pr(S \leq \tau)$ .

Next, we generalize the above expression for any  $\gamma \in \Gamma$  (not only limited to  $PR$ ), and call the average  $\gamma$  difference across thresholds *distributional disparity*, defined formally as

$$\mathcal{U}_\gamma(f) \triangleq \mathbb{E}_{\tau \sim U(\Omega)} |\gamma_g^f(\tau) - \gamma_{g'}^f(\tau)|. \quad (4)$$

We use  $\mathcal{U}_\gamma(f)$  as shorthand to denote the distributional disparity of  $f$  with respect to  $\gamma$ . With this, we can present the fairness definition that we will use to evaluate fairness across all-thresholds.

The notion of fairness we employ in this work is called *distributional parity*. Distributional parity measures the average difference in some  $\gamma \in \{PR, TPR, FPR\}$  across all possible thresholds, where the absence of distributional disparity implies distributional parity. In both definitions, we chose the uniform distribution over thresholds given that no particular threshold holds more *weight* than another, as we assume in the downstream setting, each threshold is equally likely <sup>2</sup>.

**Definition 3.1.** A regressor  $f$  satisfies **distributional parity** with respect to  $\gamma$  if

$$\mathbb{E}_{\tau \sim U(\Omega)} |\gamma_g^f(\tau) - \gamma_{g'}^f(\tau)| = 0 \quad (5)$$

If distributional parity is achieved, then  $\gamma_g^f(\tau) = \gamma_{g'}^f(\tau)$  for all  $\tau$ , achieving the type of all-threshold guarantee we seek. Note that distributional parity is defined with respect to a single  $\gamma$ , and not *all* rates at once. We will show later on that our post processing method works for weighted combinations of rates, allowing the practitioner to recover fairness notions that consider multiple rates at once like equalized odds, or could even be extended to encompass cost-weighted notions of fairness which have recently received attention [ABD<sup>+</sup>18].

### 3.1 Distributional Parity and Label-Dependent Metrics

To demonstrate why distributional parity is the correct approach for achieving all-thresholds fairness, we will first show how a special case of distributional parity has been achieved for label-*independent* metrics (namely positive rates), and then explain why this approach cannot be extended to the label-dependent case (Equalized Odds or Equal Opportunity). Our goal in this section is to highlight this limitation in hopes that it will motivate our geometric repair based approach, as outlined in Section 4.

For the label-independent case, i.e. when  $\gamma = PR$ , satisfying positive rate parity at all thresholds has previously been referred to as Strong Demographic Parity [JPS<sup>+</sup>20, CDH<sup>+</sup>20a]:

**Definition 3.2.** A regressor  $f$  satisfies **strong demographic parity** (SDP) if

$$\mathbb{E}_{\tau \in U(\Omega)} |PR_g^f(\tau) - PR_{g'}^f(\tau)| = 0. \quad (6)$$

In [CDH<sup>+</sup>20a, GLR20], the authors show that a regressor which satisfies the following constraint, satisfies strong demographic parity.

**Proposition 2.** A regressor  $f$  satisfies strong demographic parity if for all  $(x, g)$  it holds that

$$F_g(s) = F_{g'}(s) \quad \text{where } f(x, g) = s \quad (7)$$

For convenience, we'll refer to such an  $f$  as  $f^{SDP}$ . This proposition shows that *SDP* is satisfied when all scores belong to the percentile in each groupwise score distribution, or in other words, when scores are identically distributed.

From this, we learn that identifying the percentiles of each group distribution is an important requirement to enforcing strong demographic parity. Once these percentiles can be computed, the trick to satisfying this condition is to compute some score-wise *shift*, such that percentiles across groups align. In fact, this shift is exactly the transformation required to transform  $f$ 's output to that of  $f^{SDP}$ .

As is desired in our downstream setting these works show how to compute  $f^{SDP}$  using post-processing. This means that given any existing regressor there exists a group-aware transformation  $T^{SDP}$  such that  $T^{SDP}(f(x, g), g) = f^{SDP}(x, g)$ .

---

<sup>2</sup>For ease of exposition, our results conservatively assume a uniform distribution over thresholds. Including a non-uniform prior over threshold's usage, or equivalently a weight function over equally-likely thresholds' downstream value, would be straightforward.

**Remark 3.1.** This transformation can be computed in closed-form [CDH<sup>+</sup>20a]:

$$T^{SDP}(s, g) = p_g s + (1 - p_g) F_{g'}^{-1}(F_g(s)). \quad (8)$$

where  $p_g = p(\mathbf{G} = g)$  and ensures that the change in scores are proportional to the size of the groups.

A quick computation verifies that this transformation achieves strong demographic parity through a "percentile matching" procedure: take scores  $s_1, s_2$  s.t.  $F_g(s_1) = F_{g'}(s_2)$ , then one can derive that  $T^{SDP}(s_1, g) = T^{SDP}(s_2, g')$ . This proves that  $T^{SDP}$  can make the output any regressor satisfy strong demographic parity condition as per Proposition 2. Unfortunately, there are several reasons this approach does not extend to the label-dependent case.

To achieve distributional parity for label-dependent metrics, we need knowledge of  $Y$ , which is typically unknown at post-processing time. This is because at post-processing time, if the ground-truth was known (or even a good proxy), classification would not be needed. Suppose for example, we could compute a true positive rate post-processing transformation  $T^{TP}$  in a fashion similar to  $T^{SDP}$  as described above. Similarly, this would require knowledge of a score's percentile in the true positive distribution  $\mathbf{S}_g | \mathbf{Y}$ , such that the correct "percentile-matching" strategy can be applied, ensuring that true positive scores are similarly distributed after post-processing. Without knowledge of  $Y$ , however, we cannot identify these percentiles, making the above strategy inapplicable for label-dependent post-processing. We now re-state our problem: **how can we compute a label-dependent post-processing transformation that does not require knowledge of labels  $Y$ ?**

### 3.2 Additional Related Work

As discussed above, our approach is most closely related to [JPS<sup>+</sup>20, CDH<sup>+</sup>20b, GLR20] who achieve strong demographic parity through post processing; however, these works do not extend their approach to other metrics. [FFM<sup>+</sup>15, GDBFL19] apply geometric repair (referred to as partial repair in their work) to algorithm *inputs*, as a pre-processing method. In [YBS19] authors use the Wasserstein distance as a measure for fairness and leverage it as an in-processing method. In [CS20] geometric repair is studied from the lens of a fairness-risk trade-off, but to our knowledge, no other works apply geometric repair to the *outputs* of a model as a post-processing method for label-dependent fairness.

## 4 Geometric Repair

Our method to minimize distributional disparity is based on *geometric repair* [FFM<sup>+</sup>15, CS20, GDBFL19]. Geometric repair is a technique for computing a regressor that is *partially fair* by taking a weighted combination of an *unfair* regressor  $f$  and the *fair* regressor  $f^{SDP}$ . This combination, when parametrized by  $\lambda \in [0, 1]$ , yields a family of regressors  $\{f_\lambda\}_{\lambda \in [0, 1]}$ , where each  $f_\lambda$  is defined in the following way.

**Definition 4.1** (Geometric Repair). Let  $\lambda \in [0, 1]$  be the **repair parameter**. We define a geometrically repaired regressor  $f_\lambda$  as

$$f_\lambda(x, g) \triangleq f(x, g) + \lambda t(x, g) \quad (9)$$

where  $t$  defined as  $t(x, g) \triangleq f^{SDP}(x, g) - f(x, g)$  gives the difference between an unrepairs score and its fully repaired version.

Alternatively, we could define  $f_\lambda$  using an optimal-transport-like mapping.

**Proposition 3.** Any geometrically repaired regressor  $f_\lambda$  can be computed as the following,

$$f_\lambda(x, g) = (1 - \lambda(1 + p_g))f(x, g) + \lambda(1 - p_g)h^*(s, g)$$

where  $h^*(s, g) = F_{g'}^{-1}(F_g(s))$  is the optimal transport mapping (see Remark 2.1). Indeed,  $h^*$  behaves exactly like a transport plan in that it accepts as input a score  $s$ , determines what percentile  $s$  is in group  $g$ , and returns the score corresponding to that same percentile in group  $g'$ . The key difference between  $h^*$  and the transport plan as defined in Remark 2.1 however, is that  $h^*$  takes as input the protected group, whereas a transport plan does not.

Under these two parametrizations,  $f_{\lambda=0}$  is the original  $f$ , and  $f_{\lambda=1}$  is  $f^{SDP}$ . For this reason, we occasionally refer to  $f^{SDP}$  as the *fully repaired* regressor. The original goal of geometric repair was to parameterize a trade-off between the good performance of the original regressor  $f$ , and the fairness properties of the fully repaired regressor  $f^{SDP}$ . As we show below, geometric repair *does* successfully give a way to navigate this trade-off (which is rigorously examined in [CS20]). To the best of our knowledge however, it was not known that geometric repair gives also has the property that it can be used to compute a regressor which satisfies distributional parity, and this is our most novel contribution, which we present in Section 4.2.

## 4.1 Properties of Geometric Repair

Before presenting this result, we show that there are several properties of geometric repair which make it well suited to address the downstream fairness setting, in addition to its distributional disparity minimizing effects.

1. **Effect on Performance** - Suppose we want to bound performance of some  $f_\lambda$  under a risk minimization framework like [CS20, GLR20]. If we denote risk with  $\mathcal{R}(f_\lambda) \triangleq \|f - f_\lambda\|_1$ <sup>3</sup> then the following relationship between the risk of  $f_\lambda$  and  $f^{SDP}$  holds.

**Remark 4.1.** For any  $f_\lambda$  it holds that  $\mathcal{R}(f_\lambda) \leq \mathcal{R}(f^{SDP})$  or more specifically,

$$\mathcal{R}(f_\lambda) = \lambda \mathcal{R}(f^{SDP}) \quad \forall \lambda \in [0, 1]$$

The effect of our method on the performance (with respect to accuracy) of  $f_\lambda$  rests in analyzing the risk of  $f^{SDP}$ . As shown in [JPS<sup>+</sup>20],  $T^{SDP}$  induces the minimum number of predicted class changes on average, between  $f$  and  $f^{SDP}$ . In other words, of all transformations between the unrepairs score distributions and the repaired  $f^{SDP}$  score distributions,  $T^{SDP}$  is the transformation which increases risk the **least**. Given that  $T^{SDP}$  is the transformation used to produce  $f^{SDP}$ , the term upper-bounding the risk of  $f_\lambda$ , we see that post processing a regressor for strong demographic parity provides a common sense upper bound on the risk of repaired regressors. Additionally this relationship also makes  $\lambda$  interpretable as parametrizing the trade-off between the risk of the repaired and unrepairs regressors.

2. **Do-No-Harm** - We also show that for any  $\gamma$  that (i) there exists a closed subset of values for the repair parameter, where any repaired regressor taking with a  $\lambda$  in that subset *does not* increase distributional disparity (ii) for any  $\gamma$  there exists a (potentially different) closed set of  $\lambda$  such that distributional disparity for those regressors is at most that of  $f^{SDP}$  (iii) these subsets can overlap (which empirically, they often do) (iv) the worst case distributional disparity in the repaired family is one of  $f$  or  $f^{SDP}$ .

**Lemma 4.1.** There exists closed subsets  $\Lambda_A, \Lambda_B \subseteq [0, 1]$  with non-empty intersection s.t.  $\mathcal{U}_\gamma(f_{\lambda_a}) \leq \mathcal{U}_\gamma(f)$  for all  $\lambda_a \in \Lambda_A$ ,  $\mathcal{U}_\gamma(f_{\lambda_b}) \leq \mathcal{U}_\gamma(f^{SDP})$  for all  $\lambda_b \in \Lambda_B$ , and  $\mathcal{U}(f_\lambda) \leq \max(\mathcal{U}_\gamma(f), \mathcal{U}_\gamma(f^{SDP}))$  for all  $\lambda \in [0, 1]$ .

We call this property *Do-No-Harm*, as the above lemma shows that geometric repaired regressors are often at least as fair, if not fairer than their unrepairs or fully repaired counterparts.

3. **Rank Preserving** - We also show the  $f_\lambda$  never changes the percentiles of scores – we call this Rank Preserving-ness [FFM<sup>+</sup>15]. This property has also been called rational ordering in [LCM17]

**Proposition 4.** Any regressor is  $\{f_\lambda\}_{\lambda \in [0, 1]}$  is rank preserving, that is, for any  $\lambda \in [0, 1]$  and  $x_1, x_2$  if  $f(x_1, g) \leq f(x_2, g)$  then  $f_\lambda(x_1, g) \leq f_\lambda(x_2, g)$ .

Although geometric repair changes a regressor’s scores, this proposition illustrates that the ranking of scores, relative to one another, does not change.

In the next section, we will show how to minimize distributional disparity using geometric repair. Our technique is based in the observation that for each  $\gamma$  there is a corresponding value of the parameter  $\lambda$  that minimizes distributional disparity for that metric. Furthermore, distributional disparity is actually convex in the repair parameter, meaning that the regressor which minimizes distributional disparity is “best-in-class” amongst partially repaired regressors, or rather, is globally optimal in the regressor family.

<sup>3</sup>This result appears in both works for the  $\ell_2$  norm.

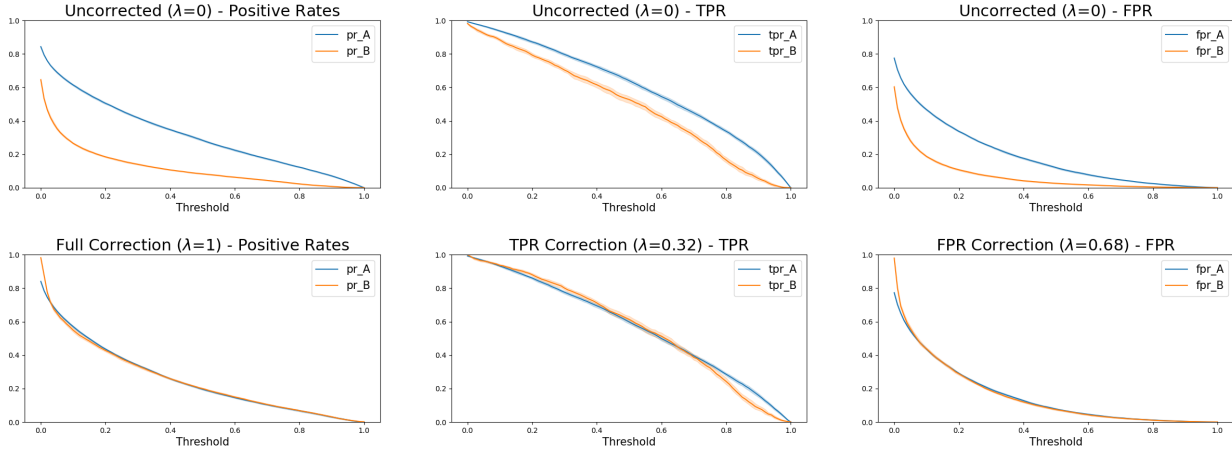


Figure 2: Experiments using the (old) Adult dataset. X-axis: all possible choices of threshold  $\tau \in [0, 1]$ . Y-axis: group-conditional selection rate, TPR, and FPR for the classifications resulting from each possible  $\tau$ . Top row: classifications based on original, uncorrected classifier probabilities. Bottom left: full correction ( $\lambda = 1$ ). Bottom middle & right:  $\lambda \approx 0.32$ ,  $\lambda \approx 0.68$ .  $\lambda$  values are calculated based on the labelled training data, and shown here applied to the unlabelled testing data.

## 4.2 Minimizing Distributional Disparity

In this section, we show that the distributional disparity metric  $\mathcal{U}_\gamma(f_\lambda)$  is convex in  $\lambda$ , indicating there is a  $\lambda^*$  such that  $f_{\lambda^*}$  minimizes distributional disparity for  $\gamma$ . At a high-level, our strategy will be to draw a connection between partially repaired regressors, their score distributions, and Wasserstein barycenters. Once this connection is made, we can easily show that fairness metrics are generally convex along barycenters (which actually form a geodesic in the Wasserstein space), and then apply this convexity result to our repaired regressors, via the correspondence that will have been established prior. We'll prove that distributional disparity is convex in  $\lambda$ , and then leverage this fact to find the  $\lambda$  and corresponding  $f_\lambda$  that minimizes distributional disparity via the proposed post-processing algorithm.

### 4.2.1 Wasserstein Geodesics

We begin at the first step, by drawing a connection between repaired regressors and their score distributions. This next proposition shows that the groupwise score distributions of a repaired regressor can be computed as Wasserstein-1 barycenters.

**Proposition 5.** For any  $\lambda \in [0, 1]$ ,  $\mathbf{S}_g^\lambda$  is distributed like the barycenter of  $\mu_{\mathbf{S}_g}, \mu_{\mathbf{S}'_g}$  with weight  $\alpha(\lambda) = (1 - \lambda(1 + p_g))$ . We denote this barycenter as  $\mu_{\mathbf{S}_g^\lambda}$  where

$$\mu_{\mathbf{S}_g^\lambda} \leftarrow \arg \min_{\nu \in \mathcal{P}_1(\Omega)} \alpha(\lambda) \mathcal{W}_1(\mu_{\mathbf{S}_g}, \nu) + (1 - \alpha(\lambda)) \mathcal{W}_1(\mu_{\mathbf{S}'_g}, \nu).$$

and so  $\mathbf{S}_g^\lambda \sim \mu_{\mathbf{S}_g^\lambda}$  (recalling that  $f_\lambda(\mathbf{X}, g)$  is distributed exactly like  $\mathbf{S}_g^\lambda$ )

Setting  $\lambda = 1$  recovers the score distribution for  $f^{SDP}$ , and setting  $\lambda = 0$  recovers the original groupwise score distributions produced by  $f$ . From this proposition, we establish that there is a 1:1 relationship between a repaired regressor, and its groupwise score distribution, which can be computed as a Wasserstein-1 barycenter. Furthermore, this implies that each  $\lambda$  yields a different pair of groupwise score distributions. We can view the enumeration of  $\lambda$  from  $0 \rightarrow 1$  as an interpolation between repaired and unrepairs score distributions, and equivalently between the output of  $f$  and  $f^{SDP}$  (from Proposition 5). In the space of probability distributions, this interpolation admits a unique and special structure. The space of distributions we consider is the Wasserstein space, and the aforementioned unique structure is that of a length minimizing path called a geodesic – we will now define the Wasserstein space and Wasserstein geodesic.

Consider a metric space  $(\mathcal{P}_1(\Omega), \mathcal{W}_1)$ <sup>4</sup> and call it the Wasserstein space denoted  $\mathcal{W}_1(\Omega)$ . We define *geodesics* in this space in the following way.

**Definition 4.2** (Geodesic in  $\mathcal{W}_1(\Omega)$ ). A curve  $\eta : [0, 1] \rightarrow \mathcal{P}_1(\Omega)$  is a geodesic<sup>5</sup> in  $\mathcal{W}_1(\Omega)$  if

$$\mathcal{W}_1(\eta(a), \eta(b)) = |a - b| \mathcal{W}(\eta(0), \eta(1))$$

With this, we can formally characterize the structure of barycenter paths in the Wasserstein space. Specifically, interpolation along barycenters produces a geodesic in  $\mathcal{W}_1(\Omega)$ , as is demonstrated via the following classical result from [San15] Theorem 5.27.

**Theorem 1.** Suppose that  $\Omega$  is convex, let  $\mu, \nu \in \mathcal{P}_1(\Omega)$  satisfy Assumption 2.1. If  $T$  is an optimal transport plan from  $\mu \rightarrow \nu$  then the set of barycenters between these distributions (as per Definition 2.1) is exactly the curve  $\mu_t = ((1-t)id + tT)_\# \mu$  where  $t \in [0, 1]$  and is a geodesic in  $\mathcal{W}_1(\Omega)$ .

A corollary of this Theorem, Proposition 5, and Definition 1, is that the set of barycenters  $\{\mu_{\mathcal{S}_g}\}_{\lambda \in [0,1]}$  produced via geometric repair *also* form a geodesic in the Wasserstein space. This is significant because in general, the Wasserstein space is not convex [AM20], except for the cases like that we study here, where we can exploit the geometry of geodesics to make special-case convexity claims.

To complete this argument, we must first revisit fairness metrics. Specifically, it will be helpful to view fairness metrics as functions which take a distribution as input (in this case,  $\mathcal{S}|\mathcal{G}, \mathcal{Y}$ ) and computes a real value, i.e. the rate  $\Pr[\mathcal{S} \geq \tau | \mathcal{G}, \mathcal{Y}]$  from it. This type of function is called a *functional over probability distributions*, and is helpful for defining the type convexity along barycenters that we've outlined so far. Next, we will formalize fairness metrics in  $\Gamma$  as functions on a probability distributions, and examine how these metrics behave along geodesics.

#### 4.2.2 Fairness Metrics as Functionals

In general, we can view fairness metrics as a functionals over the space of probabilities. Specifically, the fairness metrics we consider in this work belong to a class of functionals called the “potential energy” and are defined by the integral of a given function over some measure.

**Definition 4.3** (Potential Energy). The potential energy of a function  $V : \Omega \rightarrow \mathbb{R}$  over some measure  $\nu \in \mathcal{P}_1(\Omega)$  is defined

$$\mathcal{V}(\nu) = \int_{\Omega} V d\nu. \quad (10)$$

Let  $\mathbb{S} = \Omega \times \mathcal{G} \times \mathcal{Y}$  and  $(\mathbb{S}, \mathcal{A}, \nu)$  be a probability space. We'll use a shorthand notation like  $\mathbb{S}|\mathcal{G}, \mathcal{Y}$  to denote subsets of  $\mathbb{S}$ . For example,  $\mathbb{S}|g$  is all elements in  $\mathbb{S}$  with group  $g$ .

We'll express fairness metrics as a potential energy functional with the the familiar tools of: the indicator function, a threshold, and a regressor. For example, we can re-write the positive rate<sup>6</sup> for group  $g$  as

$$PR_g^f(\tau) = \mathbb{E}_{s \sim p_{\mathcal{S}}} [\mathbb{1}_{s \geq \tau} | \mathcal{G} = g] = \frac{1}{\Pr[\mathcal{G} = g]} \int_{\mathbb{S}|g} \mathbb{1}_{s \geq \tau} d\nu. \quad (11)$$

where the last equality follows by definition of conditional expectation. Similarly, we could express groupwise true positive rate (TPR) as

$$TPR_g^f(\tau) = \mathbb{E}_{s \sim p_{\mathcal{S}}} [\mathbb{1}_{s \geq \tau} | \mathcal{Y} = 1, \mathcal{G} = g] = \frac{1}{\Pr[\mathcal{Y} = 1, \mathcal{G} = g]} \int_{\mathbb{S}|g, 1} \mathbb{1}_{s \geq \tau} d\nu. \quad (12)$$

To be general, we will notate any positive rate produced by conditioning on some event  $Z$  as

$$\gamma_g^f(\tau) = \mathbb{E}_{s \sim p_{\mathcal{S}}} [\mathbb{1}_{s \geq \tau} | Z] = \frac{1}{\Pr[Z]} \int_{\mathbb{S}|Z} \mathbb{1}_{s \geq \tau} d\nu. \quad (13)$$

<sup>4</sup>it is well known that the Wasserstein Distance is a metric

<sup>5</sup>Most precisely, this is the definition for a constant-speed geodesic.

<sup>6</sup>The existence of these conditional expectations is established by the absolute continuity of  $\nu$  and subsequently the Radon Nikodym Theorem.

Finally, in the next subsection, we characterize the convexity of these functionals under geometric repair, which under this formulation, is equivalent to characterizing the convexity of these functionals along geodesics in the Wasserstein space. Convexity along Wasserstein geodesics is called displacement convexity and was originally proposed by [McC97].

### 4.2.3 Displacement Convexity

Conceptually, displacement convexity describes the phenomena that some functional on probability measures is convex as one interpolates between two distributions, along their barycenters – recall that these barycenters form a geodesic (Theorem 1). Since the interpolation of score distributions via geometric repair produces a Wasserstein geodesic, displacement convexity is a tool well suited to help us characterize the convexity of fairness metrics under geometric repair.

**Definition 4.4** (Displacement Convex). A functional  $\mathcal{V} : \mathcal{P}_1(\Omega) \rightarrow \mathbb{R}$  is said to be displacement convex if the mapping  $t \mapsto \mathcal{V}(\mu_t)$  is convex where  $\mu_t = ((1-t)id + tT)\#\mu$  is a geodesic between any  $\mu, \nu \in \mathcal{P}_1(\Omega)$  and  $T$  is the transport plan from  $\mu \rightarrow \nu$ <sup>7</sup>

The following theorem provides a necessary and sufficient condition to determine if potential energy functional is displacement convex. Unsurprisingly, the displacement convexity of the functional  $\mathcal{V}$  rests entirely on the convexity of the function  $V$  that it integrates over.

**Theorem 2.** The functional  $\mathcal{V}$  is displacement convex iff  $V$  is convex ([San15] Proposition 7.25; [AC11] Proposition 7.7)

In the case of fairness metrics, the function  $V$  is the indicator function over scores – producing  $\hat{Y} = 1$  at some  $\tau$  i.e.  $\mathbb{1}_{[\tau,1]}$ . In general, the indicator function is convex over convex sets [Fré17]. Clearly,  $[\tau, 1]$  is a convex set, making the indicator function a convex function. From this, we can easily establish that  $\gamma(\cdot)$  is displacement convex (Definition 4.4) with the following Lemma.

**Lemma 4.2.** Any metric  $\gamma \in \Gamma$  is displacement convex. Additionally, if  $\vec{\alpha} \in \mathbb{R}_{\geq 0}^d$  such that  $\sum_{i=1}^d \alpha_i = 1$  and  $\gamma_1 \dots \gamma_d \in \Gamma$  then  $\sum_{i=1}^d \alpha_i \gamma_i$  is displacement also convex.

From this Lemma we see that fairness metrics are displacement convex, which is essential to show that  $\mathcal{U}_\gamma$  is also displacement convex, given that it is simply a composition of  $\gamma$ 's. We state this result formally with the following theorem.

**Theorem 3.** With respect to any  $\gamma$ , the distributional disparity mapping  $\lambda \mapsto \mathcal{U}_\gamma(f_\lambda)$  is convex (in  $\lambda$ ).

The convexity of  $\lambda \mapsto \mathcal{U}_\gamma(f_\lambda)$  implies that there is a  $\lambda^*$  and corresponding  $f_{\lambda^*}$  which minimizes  $\mathcal{U}_\gamma(f_\lambda)$  in the space of repaired regressors (and their barycenters). Next we give an algorithm for finding  $\lambda^*$  for a given  $\gamma$ .

### 4.2.4 Post-Processing for Distributional Parity

Now we describe our proposed post-processing algorithm for minimizing distributional disparity. The goal of our method is to take an unrepairs regressor  $f$  and a fair regressor  $f^{SDP}$  and find some combination of the two functions via geometric repair (Definition 4.1) such that the combination, which is some  $f_\lambda$  belonging to the family  $\{f_\lambda\}_{\lambda \in [0,1]}$ , minimizes distributional disparity for a single metric, or combination of metrics in  $\Gamma$ . Since the set of regressors produced by such a combination are parameterized by repair parameter  $\lambda$ , our goal reduces to finding the  $\lambda$  which best minimizes distributional disparity i.e. the  $\lambda$  that minimizes  $\mathcal{U}_\gamma(f_\lambda)$  for some  $\gamma$ . The distributional disparity minimizing parameter  $\lambda^*$  can be found

$$\lambda^* \leftarrow \arg \min_{\lambda \in [0,1]} \mathcal{U}_\gamma(f_\lambda) \quad \text{with} \quad \mathcal{U}_\gamma(f_\lambda) = \mathbb{E}_{\tau \sim U(\Omega)} |\gamma_g^{f_\lambda}(\tau) - \gamma_{g'}^{f_\lambda}(\tau)|.$$

and subsequently, the regressor which satisfies distributional parity is  $f_{\lambda^*}$ .

---

<sup>7</sup>This definition is from ([AC11] Definition 7.2)

	Adult Income-Sex		Adult Income -Race		Public Coverage		Taiwan Credit	
	TPR	EO	TPR	EO	TPR	EO	TPR	EO
Uncorrected	0.218	0.391	0.116	0.161	0.058	0.190	0.121	0.173
Jiang/Chzhen	0.408	0.442	0.173	0.213	0.061	0.081	0.089	0.094
<b>Ours - TPR</b>	<b>0.139</b>	<b>0.228</b>	<b>0.072</b>	<b>0.182</b>	<b>0.047</b>	<b>0.117</b>	<b>0.060</b>	<b>0.080</b>
Pleiss - TPR	0.279	0.296	0.215	0.234	0.127	0.173	0.337	0.383
Feldman - TPR	0.192	0.373	0.344	0.592	0.343	0.592	0.344	0.592
<b>Ours - Eq Odds</b>	<b>0.124</b>	<b>0.228</b>	<b>0.068</b>	<b>0.182</b>	<b>0.047</b>	<b>0.077</b>	<b>0.060</b>	<b>0.079</b>
Pleiss - Eq Odds	1.00	1.487	0.131	0.131	0.172	0.227	0.894	1.246
Feldman - Eq Odds	0.192	0.373	0.344	0.592	0.344	0.592	0.344	0.592

Table 1: Worst-case disparities (in TPR & EO) at *any* threshold for each dataset & algorithm. Closer to zero is better.

To compute this optimal  $\lambda^*$  we use Algorithm 1. At a high level, our algorithm simply searches over possible  $\lambda$ 's to find the one that empirically minimizes distributional parity on available data. Fortunately,  $\lambda^*$  is easy to locate using standard out of the box search algorithms for univariate optimization.<sup>8</sup> To make the objective tractable, and ready for search, we estimate all probabilities/expectations empirically with some sampled data, and  $\gamma$  are estimated at a finite number of equally spaced thresholds. Our approach is detailed in Algorithm 1.

---

**Algorithm 1** Distributional Parity Post-Processing

---

**Input:** A labeled dataset  $D = \{(x_i, g_i, y_i)\}_{i=1}^M$ , an unlabeled dataset  $C = \{(x_i, g_i)\}_{i=1}^N$ , and regressor  $f(x, g)$ , and  $\gamma \in \Gamma$   
 Compute  $f_{SDP}$  from  $C$  as in Eq (8).  
 Partition  $D = D_g \cup D_{g'}$  by protected group  
 Let  $\mathcal{U} = \{f(x_i, g_i)\}_{i \in |C|}$  be the unique scores of  $f_{SDP}$   
 Compute  $\lambda^* \leftarrow \text{minsearch}_{\lambda \in [0,1]} (\sum_{\tau \in \mathcal{U}} |\gamma_g^{f_\lambda}(\tau) - \gamma_{g'}^{f_\lambda}(\tau)|)$   
 where  $\gamma_g^{f_\lambda}(\tau) = \sum_{(x,g) \in D_g} \mathbb{1}_{f_\lambda(x,g) \geq \tau}$  (depending on  $\gamma$ , also restrict elements based on  $Y$ )  
**Output:**  $\{f_{\lambda^*}(x, g)\}_{(x,g) \in C}$  i.e. Apply  $f_{\lambda^*}$  on unlabeled  $C$  to obtain repaired scores

---

## 5 Experiments

To demonstrate our approach in achieving distributional parity in unlabeled data, we evaluate Algorithm 1 on several datasets. Additional experimental details can be found in the appendix. We split each dataset into three equal parts: one for training the underlying classifier, one for the labeled dataset in the input to Algorithm 1, and one for the unlabeled dataset in the input to Algorithm 1. We produce *fusing* a scikit-learn random forest with default hyperparameters. Given predictions from the trained random forest, we use the labeled portion of the dataset to calculate the optimal repair parameter(s)  $\lambda$ .

**Metrics and evaluation.** We run ten trials for each experiment, each with a train-val-test split based on a different random seed. In our experiments, we measure disparities in TPR, FPR, and EqOdds across all thresholds  $\tau \in \{0, 0.01, 0.02, \dots, 0.99, 1\}$ . We implement EqOdds as the sum of TPR and FPR differences as per Lemma 4.2. We visualize these rates at every threshold to verify our all-threshold claim (Figures 2,3). Results from [JPS<sup>+</sup>20, CDH<sup>+</sup>20b] show a special case of our postprocessing approach with  $\lambda = 1$  minimizes  $\mathcal{U}_{PR}$ , so we omit positive rate disparities from the following section.

**Baselines.** In addition to comparing our approach to the original, uncorrected classifier, we also compare the performance of our algorithm against the following methods: **Jiang/Chzhen** [JPS<sup>+</sup>20, CDH<sup>+</sup>20b], i.e. our approach with  $\lambda = 1$ . **Feldman** et.al. [FFM<sup>+</sup>15], a preprocessing method which applies a similar

<sup>8</sup>We note that  $\mathcal{U}_\gamma(\cdot)$  is convex and so standard convex optimization tools can also be used to locate the optimal repair parameter, however we find in our case that lightweight optimization algorithms were equally effective - we used `scipy.minimize_scalar`. To this end, the derivative of  $\mathcal{U}$  is computed in the appendix

geometric repair approach, but to algorithm *inputs* instead of *outputs*. Feldman also includes a tunable parameter **repairlevel** which is similar to our  $\lambda$ ; we tested repair levels in  $\{0.1, 0.2, \dots, 0.9, 1.0\}$  and show results from the best repair level for each metric. **Pleiss** et.al. [PRW<sup>+</sup>17], a post-processing method which seeks to achieve calibrated scores for all groups. Pleiss also includes options to optimize for a variety of metrics, including TPR and EO. We compare our TPR-optimized outputs with those from TPR-optimized Feldman and TPR-optimized Pleiss, and the same for EqOdds. For **Pleiss** and **Feldman**, we adapt implementations available from IBM AIF360 [BDH<sup>+</sup>18].

**Datasets.** We show results for the following datasets: **Adult Income - Sex (IN-S)**, the original version of the Adult Census dataset from UCI [DG17], where the sensitive attribute is Sex and target variable is income over \$50,000; **Adult Income - Race (IN-R)**, from [DHMS21], where the sensitive attribute is race; **Public Coverage (PC)**, also from [DHMS21], where the sensitive attribute is race and the target variable is whether an individual uses public health insurance; and **Taiwan Credit (TC)**, where the sensitive attribution is education level and the target variable is good credit [BKPS00].<sup>9</sup>

## 5.1 Results

**Efficacy of Algorithm 1.** Figure 2 illustrates the high-level before-and-after of our approach on the Adult Income - Sex dataset. The top row, showing results for uncorrected probabilities, shows disparities in PR, TPR, and FPR, regardless of choice of threshold; the second row shows that these disparities can be nearly eliminated with the proper choices of  $\lambda$ . Figure 3 shows a more comprehensive summary of these results over all four datasets; in each dataset, our method most consistently achieves close to zero distributional disparity for both TPR and EO, i.e. minimizes  $\mathcal{U}_{\gamma=TPR}$  and  $\mathcal{U}_{\gamma=EO}$ . Finally, Table 1 shows the *worst* disparities exhibited at *any* threshold for each method; again, our method at either the TPR or EqOdds  $\lambda$  outperforms the other methods.

**Existing methods do not necessarily achieve distributional parity.** From our experiments, our geometric repair approach generally outperforms the baselines for comparison. While explaining the exact reasons behind the behavior of Pleiss and Feldman over thresholds is outside the scope of this work, Figure 3 nevertheless demonstrates that the all-threshold behavior of these similarly-motivated fairness interventions are unpredictable at best, and wholly unreliable at worst: it is often the case that there are many thresholds where using an existing intervention *worsens* disparity. Still, Figure 3c suggests that it *may* be possible to find a **repairlevel** such that the **Feldman** preprocessing algorithm approximately satisfies the same desiderata as our postprocessing method, which is both theoretically interesting and practically promising. However, in the current presentation of Feldman, there is no way to determine the optimal **repairlevel** *a priori*, which means that a practitioner must sweep over all possible values, retraining the classifier each time; this practical consideration, as well as the fact that Feldman does not achieve these results consistently, is one reason we find our postprocessing approach to be promising.

## 6 Discussion

In this paper, we introduce a flexible post-processing method for minimizing distributional disparities across various definitions of fairness, and over all possible downstream choices of a classification threshold. Of course, no single method for achieving a specific metric of fairness can be expected to be universally applicable. If the threshold to be used is known ahead of time, for example, then it may be unnecessary to enforce *distributional* parity. Misapplication of our method may result in a false sense of security about the behavior of a postprocessed model. Application setting aside, several other limitations point to interesting areas of future work.

First, like most other methods currently proposed in the literature, our method relies on some stationarity assumptions between the training and the test distributions in order to be able to apply the  $\lambda$  computed from the training data to the  $\lambda$ ; future work may seek to characterize the impact of these assumptions more strongly given that we *only* operate on predicted probabilities. Second, as mentioned in Footnote 2, our current implementation and experimental results assume that the choice of any downstream threshold between  $[0,1]$  is equally likely; however, practitioners may have some a-priori knowledge about which ranges

---

<sup>9</sup>IN-S and TC use the CC BY 4.0 license, and IN-R and PC use the MIT license.

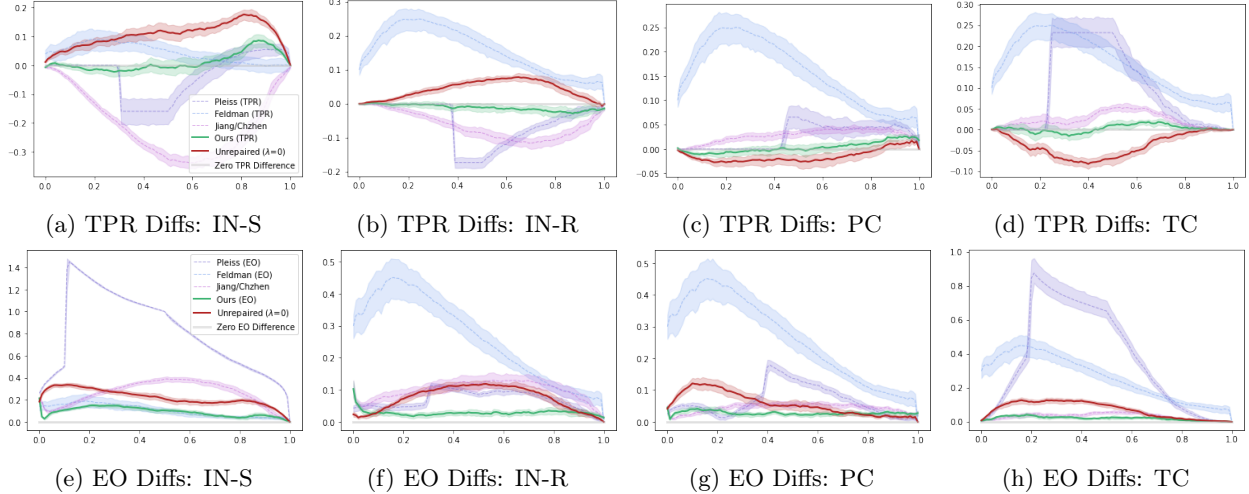


Figure 3: TPR and Equalized Odds differences  $|\gamma_g^f(\tau) - \gamma_{g'}^f(\tau)|$  across groups visualized over all thresholds  $\tau$ , for four datasets: Adult Income-Sex (IN-S), Adult Income-Race (IN-R), Public Coverage (PC), Taiwan Credit (TC). Closer to zero is better.

of thresholds are more likely, or some preferences for ranges of thresholds where distributional disparity is more costly. Future work may seek to place more emphasis on some parts of the threshold distribution than others, such as the 0.8 to 1 range in TPR from Figure 2.

Broadly, we believe this work is a practical contribution to the set of tools available to a fair machine learning practitioner. Ongoing commentary has criticized the frequent conflation of making predictions and making decisions, especially in the context of fairness [CG18, GH18]; this work is one step towards separating the two.

## References

[ABD<sup>+</sup>18] Alekh Agarwal, Alina Beygelzimer, Miroslav Dudík, John Langford, and Hanna Wallach. A reductions approach to fair classification. In *International Conference on Machine Learning*, pages 60–69. PMLR, 2018.

[AC11] Martial Aguech and Guillaume Carlier. Barycenters in the wasserstein space. *SIAM Journal on Mathematical Analysis*, 43(2):904–924, 2011.

[AM20] Anshul Adve and Alpár Mészáros. On nonexpansiveness of metric projection operators on wasserstein spaces, 2020.

[BDH<sup>+</sup>18] Rachel KE Bellamy, Kuntal Dey, Michael Hind, Samuel C Hoffman, Stephanie Houde, Kalapriya Kannan, Pranay Lohia, Jacquelyn Martino, Sameep Mehta, Aleksandra Mojsilovic, et al. Ai fairness 360: An extensible toolkit for detecting, understanding, and mitigating unwanted algorithmic bias. *arXiv preprint arXiv:1810.01943*, 2018.

[BHN19] Solon Barocas, Moritz Hardt, and Arvind Narayanan. *Fairness and Machine Learning*. fairml-book.org, 2019. <http://www.fairmlbook.org>.

[BKN<sup>+</sup>17] Amanda Bower, Sarah N. Kitchen, Laura Niss, Martin J. Strauss, Alexander Vargas, and Suresh Venkatasubramanian. Fair pipelines, 2017.

[BKPS00] Stephen D Bay, Dennis Kibler, Michael J Pazzani, and Padhraic Smyth. The uci kdd archive of large data sets for data mining research and experimentation. *ACM SIGKDD explorations newsletter*, 2(2):81–85, 2000.

[CDH<sup>+</sup>20a] Evgenii Chzhen, Christophe Denis, Mohamed Hebiri, Luca Oneto, and Massimiliano Pontil. Fair regression via plug-in estimator and recalibration with statistical guarantees. *Advances in Neural Information Processing Systems*, 33:19137–19148, 2020.

[CDH<sup>+</sup>20b] Evgenii Chzhen, Christophe Denis, Mohamed Hebiri, Luca Oneto, and Massimiliano Pontil. Fair regression with wasserstein barycenters. *arXiv preprint arXiv:2006.07286*, 2020.

[CG18] Sam Corbett-Davies and Sharad Goel. The measure and mismeasure of fairness: A critical review of fair machine learning. *CoRR*, abs/1808.00023, 2018.

[CKM<sup>+</sup>19] Jiahao Chen, Nathan Kallus, Xiaojie Mao, Geoffry Svacha, and Madeleine Udell. Fairness under unawareness. In *Proceedings of the Conference on Fairness, Accountability, and Transparency*. ACM, jan 2019.

[CKP09] Toon Calders, Faisal Kamiran, and Mykola Pechenizkiy. Building classifiers with independency constraints. In *2009 IEEE International Conference on Data Mining Workshops*, pages 13–18, 2009.

[CS20] Evgenii Chzhen and Nicolas Schreuder. A minimax framework for quantifying risk-fairness trade-off in regression, 2020.

[CW20] Mingliang Chen and Min Wu. Towards threshold invariant fair classification. In *Conference on Uncertainty in Artificial Intelligence*, pages 560–569. PMLR, 2020.

[DG17] Dheeru Dua and Casey Graff. UCI machine learning repository, 2017.

[DHMS21] Frances Ding, Moritz Hardt, John Miller, and Ludwig Schmidt. Retiring adult: New datasets for fair machine learning. *arXiv preprint arXiv:2108.04884*, 2021.

[DIJ20] Cynthia Dwork, Christina Ilvento, and Meena Jagadeesan. Individual fairness in pipelines. *CoRR*, abs/2004.05167, 2020.

[FFM<sup>+</sup>15] Michael Feldman, Sorelle A Friedler, John Moeller, Carlos Scheidegger, and Suresh Venkatasubramanian. Certifying and removing disparate impact. In *proceedings of the 21th ACM SIGKDD international conference on knowledge discovery and data mining*, pages 259–268, 2015.

[Fré17] Michel Frémond. *Collisions Engineering: Theory and Applications*. Springer, 2017.

[FSV<sup>+</sup>19] Sorelle A Friedler, Carlos Scheidegger, Suresh Venkatasubramanian, Sonam Choudhary, Evan P Hamilton, and Derek Roth. A comparative study of fairness-enhancing interventions in machine learning. In *Proceedings of the conference on fairness, accountability, and transparency*, pages 329–338, 2019.

[GDBFL19] Paula Gordaliza, Eustasio Del Barrio, Gamboa Fabrice, and Jean-Michel Loubes. Obtaining fairness using optimal transport theory. In *International Conference on Machine Learning*, pages 2357–2365. PMLR, 2019.

[GH18] Ben Green and Lily Hu. The myth in the methodology: Towards a recontextualization of fairness in machine learning. In *Proceedings of the machine learning: the debates workshop*, 2018.

[GLR20] Thibaut Le Gouic, Jean-Michel Loubes, and Philippe Rigollet. Projection to fairness in statistical learning. *arXiv preprint arXiv:2005.11720*, 2020.

[HC20] Lily Hu and Yiling Chen. Fair classification and social welfare. *FAT\* '20*, page 535–545, New York, NY, USA, 2020. Association for Computing Machinery.

[Hof19] Anna Lauren Hoffmann. Where fairness fails: data, algorithms, and the limits of antidiscrimination discourse. *Information, Communication & Society*, 22(7):900–915, 2019.

[HPS16] Moritz Hardt, Eric Price, and Nathan Srebro. Equality of opportunity in supervised learning. In *Proceedings of the 30th International Conference on Neural Information Processing Systems*, pages 3323–3331, 2016.

[JPS<sup>+</sup>20] Ray Jiang, Aldo Pacchiano, Tom Stepleton, Heinrich Jiang, and Silvia Chiappa. Wasserstein fair classification. In *Uncertainty in Artificial Intelligence*, pages 862–872. PMLR, 2020.

[LCM17] Zachary C. Lipton, Alexandra Chouldechova, and Julian McAuley. Does mitigating ml’s impact disparity require treatment disparity?, 2017.

[McC97] Robert J. McCann. A convexity principle for interacting gases. *Advances in Mathematics*, 128(1):153–179, 1997.

[PRW<sup>+</sup>17] Geoff Pleiss, Manish Raghavan, Felix Wu, Jon Kleinberg, and Kilian Q Weinberger. On fairness and calibration. *Advances in Neural Information Processing Systems*, 30:5680–5689, 2017.

[PSRA<sup>+</sup>20] Nathan Peiffer-Smadja, Timothy Miles Rawson, Raheelah Ahmad, Albert Buchard, P Georgiou, F-X Lescure, Gabriel Birgand, and Alison Helen Holmes. Machine learning for clinical decision support in infectious diseases: a narrative review of current applications. *Clinical Microbiology and Infection*, 26(5):584–595, 2020.

[San15] Filippo Santambrogio. Optimal transport for applied mathematicians. *Birkhäuser*, NY, 55(58–63):94, 2015.

[SBF<sup>+</sup>19] Andrew D. Selbst, Danah Boyd, Sorelle A. Friedler, Suresh Venkatasubramanian, and Janet Vertesi. Fairness and abstraction in sociotechnical systems. In *Proceedings of the Conference on Fairness, Accountability, and Transparency*, *FAT\* '19*, page 59–68, New York, NY, USA, 2019. Association for Computing Machinery.

[YBS19] Mikhail Yurochkin, Amanda Bower, and Yuekai Sun. Training individually fair ml models with sensitive subspace robustness. *arXiv preprint arXiv:1907.00020*, 2019.

[ZVR<sup>+</sup>17] Muhammad Bilal Zafar, Isabel Valera, Manuel Gomez Rodriguez, Krishna P. Gummadi, and Adrian Weller. From parity to preference-based notions of fairness in classification, 2017.

## A Helping Results

**Lemma A.1.** Let  $\mu_{S_g^\lambda} := ((1 - \lambda)id + \lambda T)\#\mu_{S_g}$  be a geodesic between  $\mu_{S_g}, \mu_{S_{g'}}$  which are the groupwise score distributions of  $f$  for groups  $g, g'$  with transport plan  $T$  which maps from  $\mu_{S_g}$  to  $\mu_{S_{g'}}$ . If we let  $\psi_\lambda(x) = (1 - \lambda)id(x) + \lambda T(x)$  and  $\ell$  be the Lebesgue measure then the derivative of  $\gamma_g^{f_\lambda}$  is

$$\frac{d}{d\lambda} \gamma_g^{f_\lambda}(\tau) = \int_{\psi_\lambda^{-1}([\tau, 1])} \left( \frac{d\mu}{d\ell} \right) \frac{d}{d\ell} \psi_\lambda d\ell - \tau \left( \frac{d\mu}{d\ell} \right) \frac{d}{d\lambda} \psi_\lambda^{-1}(\tau) + \left( \frac{d\mu}{d\ell} \right) \frac{d}{d\lambda} \psi_\lambda^{-1}(1)$$

**Proposition 6** (Continuity of V Functionals). Proposition 7.1 from [San15]. If  $V$  is a continuous bounded function on  $\Omega$  then  $\mathcal{V}$  (as in Def. 4.3) is continuous for the weak convergence of probability measures.

**Lemma A.2.** Lemma 6 from [JPS<sup>+</sup>20]. Let  $\mu, \nu \in \mathcal{P}_1(\Omega)$  be non-atomic then

$$\int_0^1 |F_\mu(x) - F_\nu(x)| dx = \int_0^1 |F_\mu^{-1}(y) - F_\nu^{-1}(y)| dy. \quad (14)$$

**Proposition 7.** This is Proposition 1.3 from [McC97]. Let  $\mu, \nu \in \mathcal{P}_1(\Omega)$  be absolutely continuous and let  $\mu_t$  be an geodesic from  $\mu \rightarrow \nu$  as in Definition 1, Then  $\mu_t = \nu_{1-t}$  and  $\mu_t$  is absolutely continuous.

## B Proofs

### B.1 Proof of Proposition 1

The Wasserstein-1 distance (1) between two distributions measures is exactly equal to the average difference in positive rates between those distributions, averaged uniformly across all thresholds. Formally,

$$\mathcal{W}_1(\mu_{S_g}, \mu_{S_{g'}}) = \mathbb{E}_{\tau \sim U(\Omega)} |PR_g^f(\tau) - PR_{g'}^f(\tau)| \quad (15)$$

where  $U(\Omega)$  denotes the uniform distribution.

*Proof.* Recall by definition that

$$\gamma_g^f(\tau) = \Pr[\mathbf{S} \geq \tau | \mathbf{G} = g] \quad (16)$$

$$= \Pr[f(\mathbf{X}, g) \geq \tau | \mathbf{Y} = y, \mathbf{G} = g] \quad (17)$$

$$= 1 - \Pr[f(\mathbf{X}, g) \leq \tau | \mathbf{Y} = y, \mathbf{G} = g] \quad (18)$$

$$= 1 - F_g(\tau) \quad (19)$$

Substituting this into the original expectation in (14) yields

$$\mathbb{E}_{\tau \sim U(\Omega)} |\gamma_g^f(\tau) - \gamma_{g'}^f(\tau)| = \int_{\Omega} |\gamma_g^f(\tau) - \gamma_{g'}^f(\tau)|^p d\tau \quad (20)$$

$$= \int_{\Omega} |(1 - F_g(\tau)) - (1 - F_{g'}(\tau))| d\tau \quad (21)$$

$$= \int_{\Omega} |F_g(\tau) - F_{g'}(\tau)| d\tau \quad (22)$$

$$= \int_0^1 |F_g^{-1}(t) - F_{g'}^{-1}(t)| d\lambda = \mathcal{W}_1(\mu_{S_g}, \mu_{S_{g'}}) \quad (23)$$

where the second to last equality follows from lemma A.2.  $\square$

## B.2 Proof of Proposition 2

A regressor  $f$  satisfies strong demographic parity if for all  $(x, g)$  it holds that

$$F_g(s) = F_{g'}(s) \quad \text{where } f(x, g) = s \quad (24)$$

*Proof.* Strong Demographic Parity is by definition

$$\mathbb{E}_{\tau \in U(\Omega)} |PR_g^f(\tau) - PR_{g'}^f(\tau)|$$

If we recall  $PR_g^f = 1 - F_g(\tau)$  then the above can be re-written

$$\int_{\Omega} |(1 - F_g(\tau)) - (1 - F_{g'}(\tau))| d\tau$$

If we let  $F_g = F_{g'}$  then the above expression is exactly 0, indicating that  $f$  satisfies SDP.  $\square$

## B.3 Proof of Proposition 3

Any geometrically repaired regressor  $f_{\lambda}$  can be computed as the following:

$$f_{\lambda}(x, g) = (1 - \lambda + \lambda p_g) f(x, g) + \lambda(1 - p_g) h^*(s, g) \quad (25)$$

where  $h^*(x, g) = F_{g'}^{-1}(F_g(s))$  determines what percentile a score  $s$  is in group  $g$ , and returns the score corresponding to that same percentile in group  $g'$ .

*Proof.* A geometrically repaired regressor is of the form  $f(x, g) + \lambda t(x, g)$ . If we substitute  $t(x, g) = f^{SDP}(x, g) - f(x, g)$  in this expression we obtain

$$f(x, g) + \lambda t(x, g) = \quad (26)$$

$$f(x, g) + \lambda(f^{SDP}(x, g) - f(x, g)) = \quad (27)$$

$$(1 - \lambda)f(x, g) + \lambda f^{SDP}(x, g) = \quad (28)$$

$$\underbrace{(1 - \lambda)f(x, g) + \lambda(p_g f(x, g) + (1 - p_g) h^*(x, g))}_{\text{apply definition of } f^{SDP}} = \quad (29)$$

$$(1 - \lambda + \lambda p_g) f(x, g) + \lambda(1 - p_g) h^*(x, g) \quad (30)$$

Which is identical to the original barycenter computation, but with weight coefficients  $(1 - \lambda + \lambda p_g)$  and  $\lambda(1 - p_g)$ .  $\square$

## B.4 Proof of Remark 4.1

For any  $f_{\lambda}$  it holds that  $\mathcal{R}(f_{\lambda}) \leq \mathcal{R}(f^{SDP})$  or more specifically,

$$\mathcal{R}(f_{\lambda}) = \lambda \mathcal{R}(f^{SDP}) \quad \forall \lambda \in [0, 1] \quad (31)$$

*Proof.* By definition  $\mathcal{R}(f_{\lambda}) = \|f - f_{\lambda}\| = \|f - (f + \lambda(f^{SDP} - f))\| = \lambda \|f - f^{SDP}\| = \lambda \mathcal{R}(f^{SDP})$ . The claimed inequality easily follows.  $\square$

## B.5 Proof of Lemma 4.1

There exists closed subsets  $\Lambda_A, \Lambda_B \subseteq [0, 1]$  with non-empty intersection s.t.  $\mathcal{U}_{\gamma}(f_{\lambda_a}) \leq \mathcal{U}_{\gamma}(f)$  for all  $\lambda_a \in \Lambda_A$ ,  $\mathcal{U}_{\gamma}(f_{\lambda_b}) \leq \mathcal{U}_{\gamma}(f^{SDP})$  for all  $\lambda_b \in \Lambda_B$ , and  $\mathcal{U}(f_{\lambda}) \leq \max(\mathcal{U}_{\gamma}(f), \mathcal{U}_{\gamma}(f^{SDP}))$  for all  $\lambda \in [0, 1]$ .

*Proof.* There are many subsets  $\Lambda_a, \Lambda_b$  which satisfy the needed condition, however to prove existence, we will specifically designate two such subsets. We begin by remarking the following: from Lemma 4.2 the mapping  $\lambda \mapsto \mathcal{U}_\gamma(f_\lambda)$  is convex, which means there on the closed interval  $[0, 1]$  there exists a unique minimizer that we'll call  $\lambda_{\min}$ . By Proposition 6 this mapping is continuous. Lets define (wlog)  $\Lambda_a = [0, \lambda_{\min}]$  and  $\Lambda_b = [\lambda_{\min}, 1]$ . From the intermediate value theorem and the convexity of  $\mathcal{U}_\gamma$  it follows that  $\mathcal{U}_\gamma(f_{\lambda_a}) \leq \mathcal{U}_\gamma(f)$  and  $\mathcal{U}_\gamma(f_{\lambda_b}) \leq \mathcal{U}_\gamma(f^{SDP})$  for all choices  $\lambda_a \in \Lambda_a, \lambda_b \in \Lambda_b$ . Additionally,  $\lambda_{\min} \in \Lambda_a \cap \Lambda_b$  and so this intersection is non-empty. We prove the final claim by cases. In the first case, suppose  $\mathcal{U}(f) = \mathcal{U}(f^{SDP})$ . Then  $\Lambda_a \cup \Lambda_b = [0, 1]$  and for all  $\lambda \in [0, 1]$  we have  $\mathcal{U}(f_\lambda) \leq \mathcal{U}(f)$ . In the second case, Suppose  $\mathcal{U}(f) \leq \mathcal{U}(f^{SDP})$  (the proof follows similarly if you were to reverse this inequality). Here,  $\mathcal{U}_\gamma(f^{SDP}) \leftarrow \max(\mathcal{U}_\gamma(f), \mathcal{U}_\gamma(f^{SDP}))$  so

$$\mathcal{U}(f_{\lambda_a}) \leq \mathcal{U}(f) \leq \mathcal{U}(f^{SDP}) \quad \text{and} \quad \mathcal{U}(f_{\lambda_b}) \leq \mathcal{U}(f^{SDP}) \quad (32)$$

for all  $\lambda_a \in \Lambda_a, \lambda_b \in \Lambda_b$ , resulting in the desired inequality/  $\square$

## B.6 Proof of Proposition 4

Any regressor is  $\{f_\lambda\}_{\lambda \in [0,1]}$  is rank preserving, that is, for any  $\lambda \in [0, 1]$  and  $x_1, x_2$  if  $f(x_1, g) \leq f(x_2, g)$  then  $f_\lambda(x_1, g) \leq f_\lambda(x_2, g)$ .

*Proof.* By assumption  $\mu_g$  is non-atomic, indicating that  $F_{g'}^{-1}$  and  $F_{g'}$  are non-decreasing. Since  $h^*(x, g)$  is a composition of non-decreasing functions, it is also non-decreasing. With this in-mind, it easily follows that if  $f(x_1, g) \leq f(x_2, g)$  then  $(1 - \lambda + \lambda p_g)f(x_1, g) \leq (1 - \lambda + \lambda p_g)f(x_2, g)$  and also that  $h^*(x_1) \leq h^*(x_2)$ . Combining these two observations yields the proposition.  $\square$

## B.7 Proof of Lemma 4.2

Any metric  $\gamma \in \Gamma$  is displacement convex. Additionally, if  $\vec{\alpha} \in \mathbb{R}_{\geq 0}^d$  such that  $\sum_{i=1}^d \alpha_i = 1$  and  $\gamma_1 \dots \gamma_d \in \Gamma$  then  $\sum_{i=1}^d \alpha_i \gamma_i$  is also displacement convex.

*Proof.* Suppose that  $\gamma$  is some rate conditioned on an event  $Z$  such that  $\gamma(\tau) = \Pr(\hat{Y} = 1|Z)$ . By definition

$$\gamma(\tau) = \Pr_{s \sim p_{S|Z}} [\mathbb{1}_{s \geq \tau} | Z] = \mathbb{E}_{s \sim p_{S|Z}} [\mathbb{1}_{s \geq \tau} | Z] = \frac{1}{\Pr[Z]} \int_{\Omega|Z} \mathbb{1}_{s \geq \tau} d\nu \quad (33)$$

Let  $\Omega_{\max} := \sup(\Omega)$ . We note that set of scores where  $s \geq \tau$  is exactly  $[\tau, \Omega_{\max}]$ , which is a convex set, and so therefore the indicator  $\mathbb{1}_{s \geq \tau}$  is also convex. Applying Theorem 2 yields displacement convexity. Recalling that sums of convex functions are also convex yields displacement convexity under affine combination.  $\square$

## B.8 Proof of Lemma A.1

Let  $\mu_{S_g^\lambda} := ((1 - \lambda)id + \lambda T)\#\mu_{S_g}$  be a geodesic between  $\mu_{S_g}, \mu_{S_g'}$  which are the groupwise score distributions of  $f$  for groups  $g, g'$  with transport plan  $T$  which maps from  $\mu_{S_g}$  to  $\mu_{S_g'}$ . If we let  $\psi_\lambda(x) = (1 - \lambda)id(x) + \lambda T(x)$  and  $\ell$  be the Lebesgue measure then the derivative of  $\gamma_g^{f_\lambda}$  is

$$\frac{d}{d\lambda} \gamma_g^{f_\lambda}(\tau) = \int_{\psi_t^{-1}([\tau, 1])} \left( \frac{d\mu}{d\ell} \right) \frac{d}{d\lambda} \psi_\lambda d\ell - \tau \left( \frac{d\mu}{d\ell} \right) \frac{d}{d\lambda} \psi_\lambda^{-1}(\tau) + \left( \frac{d\mu}{d\ell} \right) \frac{d}{d\lambda} \psi_\lambda^{-1}(1)$$

*Proof.* We can write

$$\gamma_g^{f_\lambda}(\tau) = \int_{\Omega} \mathbb{1}_{s \geq \tau} d\mu_{S_g^\lambda} = \int_{[\tau, 1]} 1d(\psi_\lambda \#\mu_{S_g}) \quad (34)$$

where the first equality is by definition of  $\gamma$  and the second equality follows by definition of  $\mu_{S_g^\lambda}$ . Continuing on we obtain

$$\int_{[\tau, 1]} 1d(\psi_\lambda \#\mu_{S_g}) = \int_{\psi_t^{-1}([\tau, 1])} \psi_\lambda d\mu_{S_g} = \int_{\psi_t^{-1}([\tau, 1])} \frac{d\mu_{S_g}}{d\ell} \psi_\lambda d\ell \quad (35)$$

where the first equality comes from applying change of variables via the push-forward measure. The second equality is obtained via the Radon-Nikodym Theorem, since  $\mu$  is absolutely continuous w.r.t the Lebesgue measure  $\ell$  by assumption.

In non-measure theoretic language,  $\frac{d\mu_{S_g}}{d\ell}$  is nothing more than the pdf of  $\mu_{S_g}$ . If we make this switch (and allow  $\frac{d\mu_{S_g}}{d\ell} = p_{S_g}$ ) then the above is exactly

$$\mathbb{E}_{x \sim p_{S_g}} [\psi_t(x) \mathbb{1}_{\psi_t(x) \geq \tau}] = \mathbb{E}_{x \sim p_{S_g}} [\psi_t(x) | \psi_t(x) \geq \tau] \quad (36)$$

Continuing on, we are interesting in taking the derivative of (34). It is easy to argue that  $\psi$  is bounded (between 0 and 1), integrable with respect to the Lebesgue measure, and differentiable in  $\lambda$ , and so we can compute this derivative by an application of Leibniz Rule i.e.

$$\begin{aligned} \frac{d}{d\lambda} \int_{\psi_t^{-1}([\tau, 1])} \frac{d\mu_{S_g}}{d\ell} \psi_\lambda d\ell &= \\ \int_{\psi_t^{-1}([\tau, 1])} \left( \frac{d\mu_{S_g}}{d\ell} \right) \frac{d}{d\lambda} \psi_\lambda d\ell - \tau \left( \frac{d\mu_{S_g}}{d\ell} \right) \frac{d}{d\lambda} \psi_\lambda^{-1}(\tau) + \left( \frac{d\mu_{S_g}}{d\ell} \right) \frac{d}{d\lambda} \psi_\lambda^{-1}(1) & \end{aligned}$$

Note that  $\psi$  is non-decreasing since both  $id, T$  are non-decreasing (by 2.1) which means that  $\psi_\lambda^{-1}$  is well defined and differentiable.  $\square$

## B.9 Proof of Theorem 3

With respect to any  $\gamma$ , the distributional disparity mapping  $\lambda \mapsto \mathcal{U}_\gamma(f_\lambda)$  is convex (in  $\lambda$ ).

*Proof.* By definition of absolute value we can re-write  $\mathcal{U}_\gamma$  as

$$\mathcal{U}_\gamma(\tau) = \begin{cases} \gamma_g^{f^\lambda}(\tau) - \gamma_{g'}^{f^\lambda}(\tau) & \gamma_g^{f^\lambda}(\tau) - \gamma_{g'}^{f^\lambda}(\tau) > 0 \\ 0 & \gamma_g^{f^\lambda}(\tau) - \gamma_{g'}^{f^\lambda}(\tau) = 0 \\ \gamma_{g'}^{f^\lambda}(\tau) - \gamma_g^{f^\lambda}(\tau) & \gamma_{g'}^{f^\lambda}(\tau) - \gamma_g^{f^\lambda}(\tau) < 0 \end{cases}$$

Fix  $\lambda \in [0, 1]$  and let  $\mu_{S_g}$  be the usual score distribution(s) of  $f$ . Using Proposition 7 and the definition of  $\mu_{S_g}^\lambda$  from Proposition 5 we can re-write  $\mu_{S_{g'}^\lambda} = \mu_{S_g}^{1-\lambda}$  and  $\mu_{S_g}^\lambda = \mu_{S_{g'}^{1-\lambda}}$ . From this, it is easily established that  $\gamma_g^{f^\lambda}(\tau) = \gamma_{g'}^{f^{1-\lambda}}(\tau)$  and  $\gamma_{g'}^{f^\lambda}(\tau) = \gamma_g^{f^{1-\lambda}}(\tau)$  by the definition  $\gamma$ .

From this, we take the derivative of  $\mathcal{U}_\gamma(\tau)$  by applying Lemma A.1

$$\frac{d}{d\lambda} \mathcal{U}_\gamma(\tau) = \begin{cases} \gamma_g^{f^\lambda}(\tau) - \gamma_g^{f^{1-\lambda}}(\tau) = 2\gamma_g^{f^\lambda}(\tau) & \gamma_g^{f^\lambda}(\tau) - \gamma_{g'}^{f^\lambda}(\tau) > 0 \\ 0 & \gamma_g^{f^\lambda}(\tau) - \gamma_{g'}^{f^\lambda}(\tau) = 0 \\ \gamma_{g'}^{f^\lambda}(\tau) - \gamma_{g'}^{f^{1-\lambda}}(\tau) = 2\gamma_{g'}^{f^\lambda}(\tau) & \gamma_{g'}^{f^\lambda}(\tau) - \gamma_g^{f^\lambda}(\tau) < 0 \end{cases}$$

Because all  $\gamma$  are convex,  $\gamma'$  must be non-decreasing, and therefore  $\frac{d}{d\lambda} \mathcal{U}_\gamma(\tau)$ , defined everywhere as the sum of non-decreasing functions, is also non-decreasing. This is sufficient to claim that  $\lambda \mapsto \mathcal{U}_\gamma(\tau)$  is convex.  $\square$

## C Experimental details

### C.1 Experimental setup

For each dataset, we run ten trials of the experiment; all plots show the 95% confidence interval given results from all ten trials. In each trial, we set a new random seed (so that `seed=1` iff `trial=1`). Each trial proceeds as follows:

	Sens.	Attr	Prediction Task	Source
Adult (Old)		Sex	High income	UCI
Income		Race	High income	New Adult
Public Coverage		Race	Medicare	New Adult
Employment		Sex	Employed	New Adult
Taiwan Credit		Education	Good Credit	UCI
German Credit		Age	Good Credit	UCI

Table 2: Summary of datasets used for distributional fairness experiments.

1. **Score generation.** We train our underlying model, a scikit-learn `RandomForestClassifier` with default parameters. Using the trained classifier, we predict on a separate set of data to get the *scores*. For every instance in this set, we now have information about its label, group membership, and its score. Since this is a postprocessing method, we will assume that some of this data is labeled (which we can access), and some of this data is unlabeled (which we will use to validate our method).
2. **Baseline evaluation.** To get a baseline for distributional (un)fairness, for every  $\tau \in \{0, 0.01, 0.02, \dots, 0.98, 0.99, 1.0\}$ , we calculate binary decisions using  $\tau$  as the decision threshold; then, we compute group-conditional selection rates, TPR, and FPR using these decisions.
3. **Calculating the barycenter adjustment.** Calculating the barycenter adjustment does not require access to labels, so this step can use both the labeled and unlabeled data from Step (1). We calculate the barycenter for the two groups. For this computation, we use a vectorized Python implementation of [CDH<sup>+</sup>20b]’s code. Now, for every row of data from (1), both labeled and unlabeled, we now additionally have its adjustment: a single (signed) number indicating how it should be transformed in order to lie on the barycenter.
4. **Finding the best  $\lambda$ .** Finding  $\lambda$  *does* require access to labels, so we now work only with the *labeled* dataset from (1). Each  $\lambda$  corresponds to a single distributional fairness definition, so these steps are done once for each  $\gamma \in \Gamma$ . For each row of this dataset, we have access to its label, group membership, score, and adjustment to the barycenter; then, we find  $\lambda$  according to the equation following Theorem 1.
5. **Evaluation on unlabeled data.** Our results in Figure 2 illustrate the effect of using the  $\lambda$ s found in (4c) on the *unlabeled* data. Our method makes the assumption that the labeled and unlabeled data are drawn i.i.d. from the same distribution, so it is expected (and unsurprising) that the  $\lambda$ s found using the labeled data are highly effective when applied to the unlabeled data.

## C.2 Datasets

A summary of datasets used for distributional fairness experiments can be found in the table below. For German Credit and Adult (Old), we used the postprocessed versions from [FSV<sup>+</sup>19], while New Adult datasets are from [DHMS21]. All sensitive attributes are binary, with Sex binarized as male-female, Race binarized as white-nonwhite, the Education feature binarized as low education-high education, and Age binarized as young-old.

For all New Adult datasets, data is pulled from the 2018 California 1-Year Person survey. We use the first 30000 examples. Our train-test splits are as follows: 18000 for training the random forest, and the remaining 12000 for our method, of which 6000 are part of the labeled set, and 6000 are part of the unlabeled set.

The UCI Adult dataset has 30162 examples total. We use 15000 examples for training the random forest, 7581 as the unlabeled set, and 6000 for the final unlabeled set.

The UCI Taiwan dataset has 30000 examples, and we make train-test splits identical to the New Adult datasets.

The UCI German dataset has 1000 examples. We use 500 for training the random forest, 250 as the labeled dataset, and 250 as the unlabeled dataset.

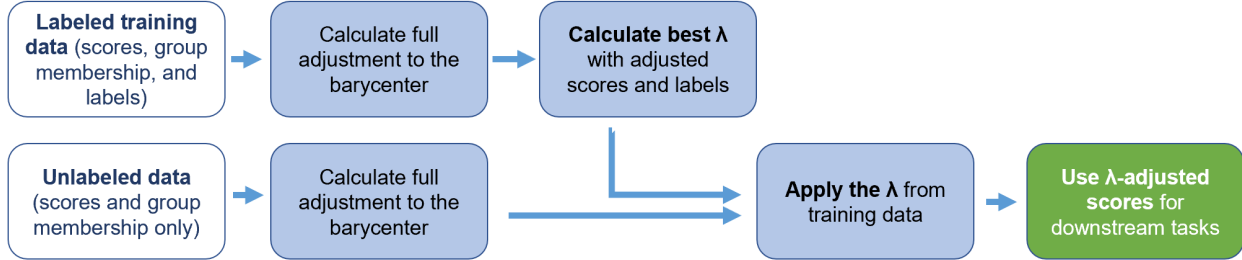


Figure 4: A summary of how each step of our post-processing method proceeds. As noted in [CDH<sup>+</sup>20b], calculating the adjustment of score distributions to the barycenter does not require ground-truth labels. Labels are only required to determine the best  $\lambda$  for the dataset given a desired metric;  $\lambda$ s are therefore calculated with the labeled training data and are used to control the barycenter adjustment for unlabeled data. Finally, note that we do not require any of the features used for the machine learning model, only group membership and the model’s predicted scores.

## D Usability

Appendix C roughly follows our anticipated workflow, illustrated in Figure 4.

Our method assumes that a reasonably-well-performing model already exists. We do not need access to the model itself—only its predictions on some labeled data. After calculating how each point’s score would need to change in order to be mapped onto the barycenter, we use that labeled data to calculate the best  $\lambda$  (or  $\vec{\lambda}$ , in case of a non-binary sensitive attribute) for a particular fairness goal (such as equal TPRs, equal FPRs, or see below for more extensions).

Meanwhile, with the unlabeled data on which we want to make adjustments, we use the model to predict scores for this data; then, we make the barycenter calculation to compute the adjustment for each point. Then, we scale those adjustments by the  $\lambda$  or  $\vec{\lambda}$  found from the labeled data. At this point, the scores have been “corrected,” and can be used in downstream applications.

By Lemma 4.2, linear combinations of the  $\gamma \in \Gamma$  that we have defined are also convex in  $\lambda$ . This means that more complex fairness goals can be achieved: for example, equalized odds by considering  $\gamma_g^{1,1}(\tau) + \gamma_g^{0,1}(\tau)$ , or even some less conventional metrics like one which considers both TPR and FPR, but weights TPR more heavily than FPR, or one which considers TPR, FPR, and PR.

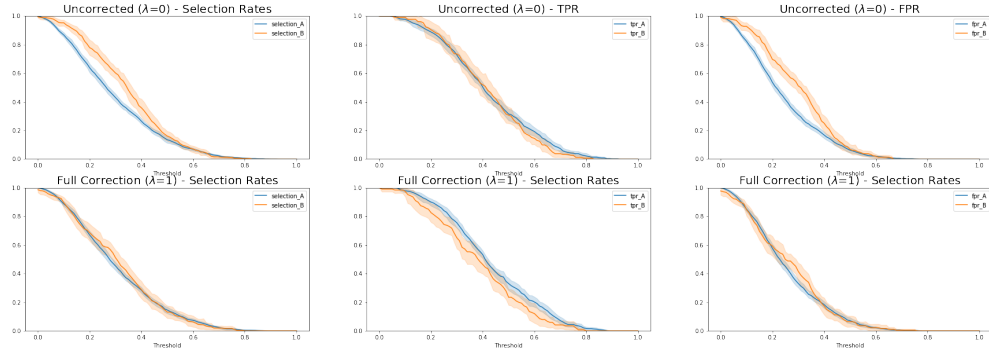
### D.1 Suitability

Our experiments hint at a few possible scenarios where our method may be less applicable: (1) when the dataset size is small; (2) when overall disparity is low; and (3) when the relationship between scores and labels is noisier for one group than another. These results suggest that in practice, it is critical to first visualize the threshold curves for both the baseline and full adjustment to determine whether our method is appropriate.

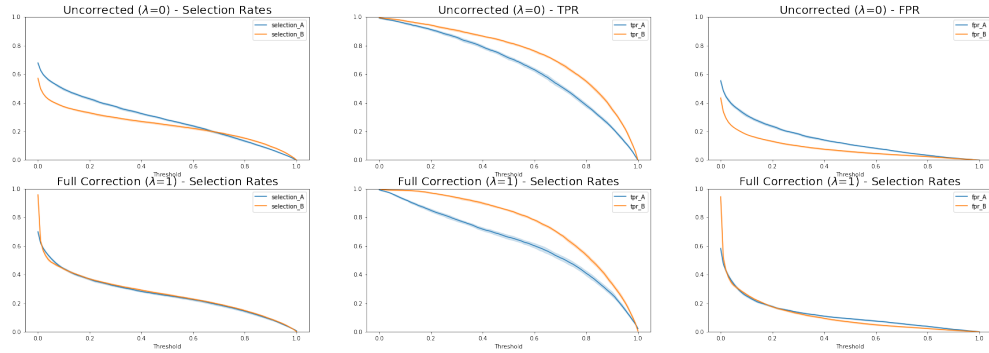
However, in industry production settings, datasets are unlikely to be small; overall low disparity is a good thing, and may mean that no intervention is strictly necessary at all; and finally, if the relationship between scores and labels is noisier for one group than another, this is an indication that the underlying regressor that produced the scores is a poor hypothesis for the learning task, which means that the model itself should be improved and that papering over its performance with a postprocessing method would be poor practice.

Here, we show results on two datasets, German and Employment, where our method does not perform as well. Figure 5 illustrates group-conditional metrics over all thresholds both before and after the full adjustment to the barycenter is applied, and Figure 7 illustrates the amount of absolute distributional disparity over all  $\lambda$ s, i.e. the same information as those in Figure 6.

**German Credit: small dataset size and low overall disparity.** First, the top row of Figure 5a shows that disparity over thresholds is quite low, even in the uncorrected case. In fact, the TPR curves are approximately overlapping. Applying the barycenter adjustment is successful—the bottom left of Figure 5a indicates that the selection rates have in fact overlapped over all thresholds. Further, note that the TPR and FPR curves, even in the full adjustment with  $\lambda = 1$ , are still extremely close. Consequently, the impact of



(a) German Credit



(b) Employment

Figure 5: Group-conditional selection rate, TPR, and FPR curves over thresholds. In each plot, the first row illustrates the uncorrected scores, and the second row illustrates the scores after full correction.

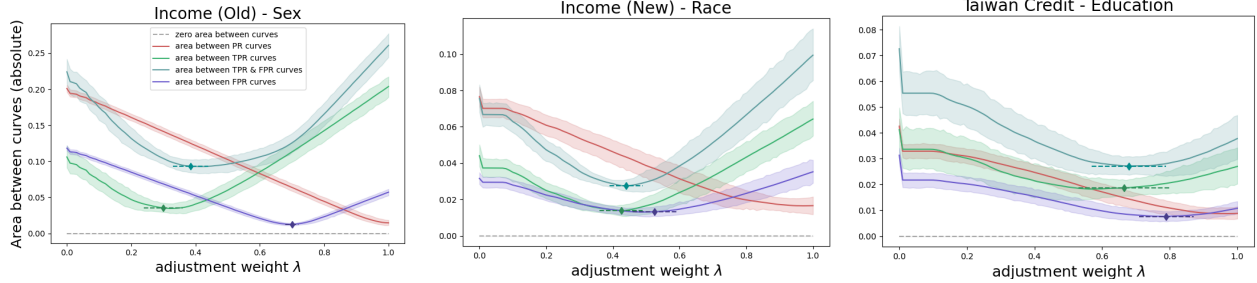


Figure 6: Each plot shows the absolute (total) area between the pairs of curves belonging to  $\gamma_g, \gamma_{g'}$  after partial repair over possible values of  $\lambda \in [0, 1]$ . The diamond marker and dashed line indicate the average and 95% confidence interval for the value of  $\lambda$  which minimizes the area between the group-conditional curves for each metric.

varying  $\lambda$ , shown in Figure 7, is extremely minimal. Furthermore, the small dataset size resulted in high variability across different train-test splits and therefore extremely wide confidence intervals. In a *single* run, results (both across thresholds and across  $\lambda$ s) were extremely noisy.

**Employment: noisy labels.** The Employment dataset, on the other hand, has plenty of samples since it is from the new Adult dataset. However, taking a closer look at the top row of Figure 5b shows that while the

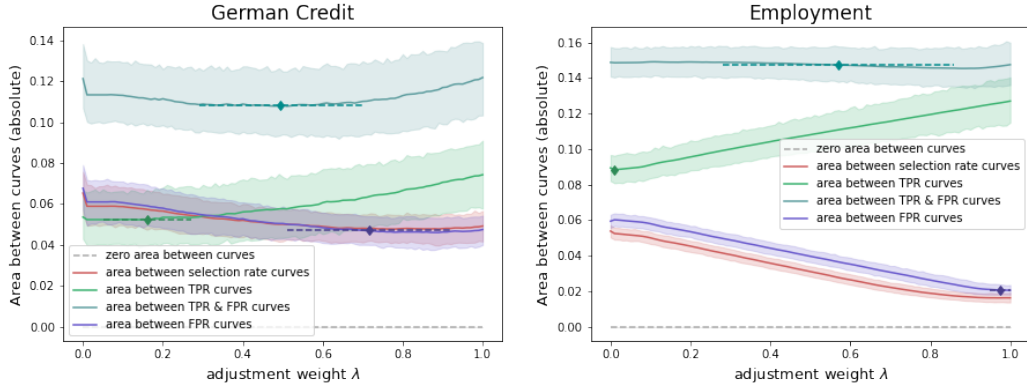


Figure 7: On the German Credit (left) and Employment (right) datasets: absolute (total) area between the pairs of curves belonging to  $\gamma_g, \gamma_{g'}$  *after partial repair* over possible values of  $\lambda \in [0, 1]$ . Note that these curves do not have the same shape as those in Figure 6: German does not show much variation in disparity across  $\lambda$ , so the minimum is fairly shallow, while the minimums for Employment fall at  $\lambda = 0$  or  $\lambda = 1$ .

selection rate and FPRs of Group A are higher than those of Group B over almost all thresholds, the TPR of Group A is *lower* than that of Group B over almost all thresholds. Contrast this with the behavior of the uncorrected scores in Figure 2, where the rates for Group A were consistently higher than Group B over all thresholds and for all three metrics. In practical terms, if Group A has a lower TPR and a higher FPR than Group B at all thresholds, this implies that the score-label relationship for Group A is much noisier than the score-label relationship for Group B, which means that merely adjusting the score distributions does not necessarily result in a strictly better or “fairer” set of results. In fact, the full correction (as shown in the bottom left of Figure 5b) is successful in that it results in identical selection rates across all thresholds, as expected, yet looking at Figure 7, it is unclear that a “true” minima for the distance between the TPR curves can be found over  $\lambda \in [0, 1]$ .